Antarctic Science 20 (5), 513–517 (2008) © Antarctic Science Ltd 2008 Printed in the UK doi:10.1017/S095410200800148X

Firn depth correction along the Antarctic grounding line

MICHIEL VAN DEN BROEKE[1]*, WILLEM JAN VAN DE BERG[1] and ERIK VAN MEIJGAARD[2]

[1]*Institute for Marine and Atmospheric Research (IMAU), Utrecht University, The Netherlands*
[2]*Royal Netherlands Meteorological Institute (KNMI), De Bilt, The Netherlands*
**m.r.vandenbroeke@uu.nl*

Abstract: To reduce the uncertainty in the calculation of Antarctic solid ice fluxes, the firn depth correction (Δh) in Antarctica is inferred from a steady-state firn densification model forced by a regional atmospheric climate model. The modelled density agrees well with observations from firn cores, apart from a site at the origin of fast flowing West Antarctic ice stream (Upstream B), where densification is anomalously rapid. The spatial distribution of Δh over Antarctica shows large variations, especially in the grounding line zone where large climate gradients exist. In places where the grounding line crosses ablation areas, Δh is zero. Along the remainder of the grounding line, Δh values range from typically 13 m in dry coastal areas (e.g. Dronning Maud Land) to 19 m in wet coastal areas (e.g. West Antarctica).

Received 8 February 2008, accepted 13 May 2008

Key words: ice sheet mass balance, sea level rise, snow compaction

Introduction

A dry firn layer of variable depth and density covers the interior ice sheets of Greenland and Antarctica. In the absence of significant melting, the steady-state firn densification rate depends mainly on temperature, accumulation rate and wind speed. In Antarctica, the firn density shows large spatial variations owing to the wide range of (near) surface climate conditions (Kaspers *et al.* 2004, Li & Zwally 2004, Zwally *et al.* 2005): in the calm, dry and cold interior, densification is slow and the firn-layer thickness can exceed 100 m. In the windier, wetter and milder coastal zone, densification is more rapid and the firn layer can be much shallower, typically 40–60 m. In regions with active katabatic winds and low precipitation rate, the firn layer can be completely removed by snowdrift erosion and/or sublimation, exposing the glacier ice at the surface (Winther *et al.* 2001, Van den Broeke *et al.* 2006).

The variable nature of the Antarctic firn layer in several ways complicates an accurate assessment of the ice sheet mass balance using the mass budget method. The greatest uncertainty arises in the calculation of the solid ice flux across the ice sheet grounding line (Rignot *et al.* 2008, Fig. 1). In the absence of direct measurements, ice thickness is usually calculated from surface elevation and a floatation criterion, which equates the mass of the displaced seawater with the added weight of the combined ice/firn column:

$$(h_i + h_f - h_{asl})\rho_{sw} = h_f\rho_f + h_i\rho_i \equiv \rho_i H_i \qquad (1)$$

where h_i, h_f and ρ_i, ρ_f are the thicknesses and average densities of the ice and firn layers, respectively, h_{asl} is the elevation of the floating glacier surface above sea level and ρ_{sw} is the density of seawater (Fig. 1). The equivalent ice thickness (H_i) is defined as the reduced total thickness obtained by compressing the firn layer until it has the density of glacier ice (~900 kg m^{-3}). H_i can be expressed in terms of h_{asl} by eliminating h_i:

$$H_i = \frac{(h_{asl} - \Delta h)\rho_{sw}}{\rho_{sw} - \rho_i}; \quad \Delta h = h_f(1 - \rho_f/\rho_i) \qquad (2)$$

where Δh is the *firn depth correction*, defined as the difference between the combined ice/firn column and the equivalent ice thickness. To convert h_{asl} to H_i, Δh must be known at the grounding line.

Density profiles from firn cores show typical Δh values ranging between 12 and 20 m. Because medium-deep firn cores that reach the firn-ice transition at 50–150 m depth are relatively scarce in Antarctica and seldom drilled at the grounding line, the spatial distribution of Δh along the grounding line is poorly known at present. As a result, Δh is often assumed constant in ice flux calculations, which introduces a considerable uncertainty. The role of uncertainty in Δh increases with decreasing ice thickness. For a typical ice thickness of 500 m, ($h_{asl} \approx 54$ m), an uncertainty in Δh of 4 m introduces a 7.4% uncertainty in the ice flux estimate. This error potentially dominates the total uncertainty in the solid ice flux. Other sources of error are the surface elevation from satellite laser altimetry (uncertainty < 0.5 m or < 1% for this example, if GLAS sensor onboard ICESAT can be used, but < 10 m or 19% for this example if ERS1/2 data must be used, Bamber & Gomez-Dans 2005) and glacier velocity from radar interferometry (< 5% uncertainty in column ice speed, Rignot *et al.* 2008).

Here, we use output of a regional atmospheric climate model to drive a steady-state firn densification model so as to obtain the distribution of Δh over the Antarctic ice sheet, including its interpolated value at the grounding line, to reduce its contribution to the uncertainty in ice flux calculations.

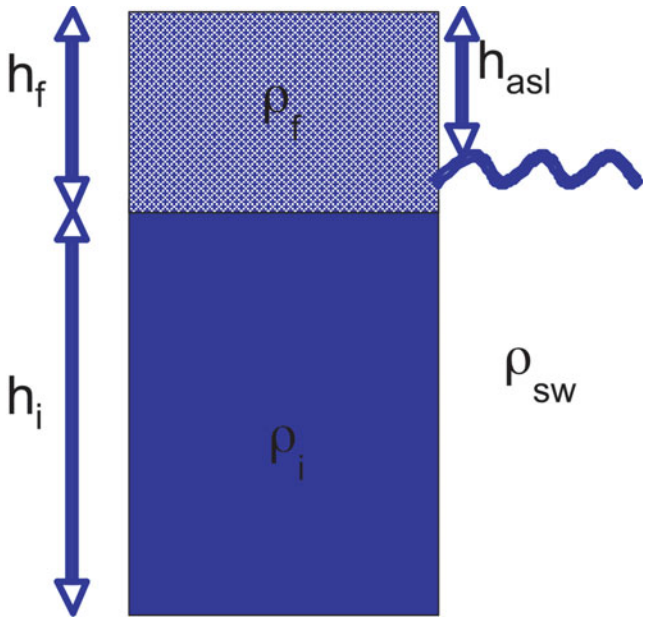

Fig. 1. Cartoon of a floating ice tongue covered with a firn layer, explanation of symbols.

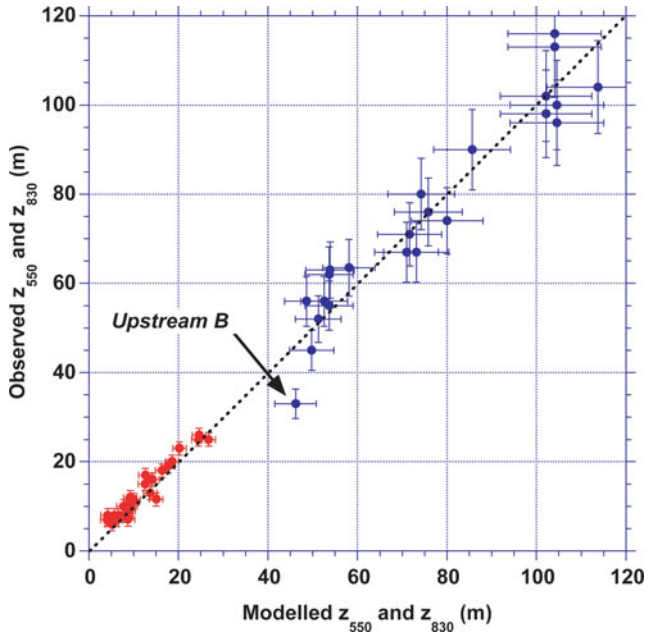

Fig. 2. Observed depth of the critical density levels 550 kg m^{-3} (red) and 830 kg m^{-3} (blue) as a function of the modelled value. Error bars in observations represent the uncertainty of the (visual) interpolation of (non-digitized) density profiles and in model values error bars represent uncertainties resulting from the spatial interpolation.

Methods

Firn densification model

Steady-state dry firn densification models have been proposed by, among others, Herron & Langway (1980), Pimienta & Duval (1987), Kameda *et al.* (1994), Arnaud *et al.* (1998), Craven & Allison (1998) and Spencer *et al.* (2001). Kaspers *et al.* (2004) tested several of these models for a wide range of Antarctic climate conditions and found good results for the models of Herron & Langway (1980), Pimienta & Duval (1987) and Arnaud *et al.* (2000). The surface density is calculated based on average surface temperature, accumulation and wind speed as modified from Kaspers *et al.* (2004). The density model is then integrated downwards from the surface to the depth where the density of glacier ice (assumed to be 900 kg m^{-3}) is reached, after which Δh is calculated from the total firn mass and depth of the firn column. We follow the approach of Barnola *et al.* (1991), who advocated the use of the Herron & Langway (1980) densification rate expressions from the surface to the first critical density level (550 kg m^{-3}), below which the expressions of Pimienta & Duval (1987) are used. We adopt the grounding line definition as used by Vaughan and others (1999), which is based on the Antarctic Digital Database. The firn densification model is forced over the entire ice sheet using output of a regional climate model at a horizontal resolution of approximately 55 km.

Atmospheric model

The expressions for the surface density and below-surface densification rate require as input values of annual average surface temperature (T_s), accumulation (A) and 10 m wind speed (V_{10}). These fields are taken as 25 year averages (1980–2004) from a regional atmospheric climate model (RACMO2/ANT). RACMO2/ANT has a horizontal resolution of 55 km and is driven at the lateral boundaries by ECMWF re-analysis (ERA40, January 1980–September 2002) and operational analysis (October 2002–December 2004). Sea ice cover and sea surface temperature are prescribed from ERA40. We use an accumulation distribution that takes in a simple fashion into account the sublimation and erosion by snowdrift (Van den Broeke *et al.* 2006). The (near) surface climate of RACMO2/ANT has been validated using measurements of T_s, A and V_{10} from various Antarctic firn core sites. Previously, Van Lipzig *et al.* (2004), Reijmer *et al.* (2005) and Van de Berg *et al.* (2006) have shown that RACMO2/ANT provides a good representation of the Antarctic near-surface climate and mass balance, which was confirmed by independent comparison at firn coring sites (Van den Broeke 2008). A cold bias of 2.2 K in modelled surface temperature is corrected prior to the density calculations.

Results

To assess the quality of the modelled density profiles, the directly observed and modelled depths of two critical density levels, 550 and 830 kg m^{-3}, are compared in Fig. 2. The first

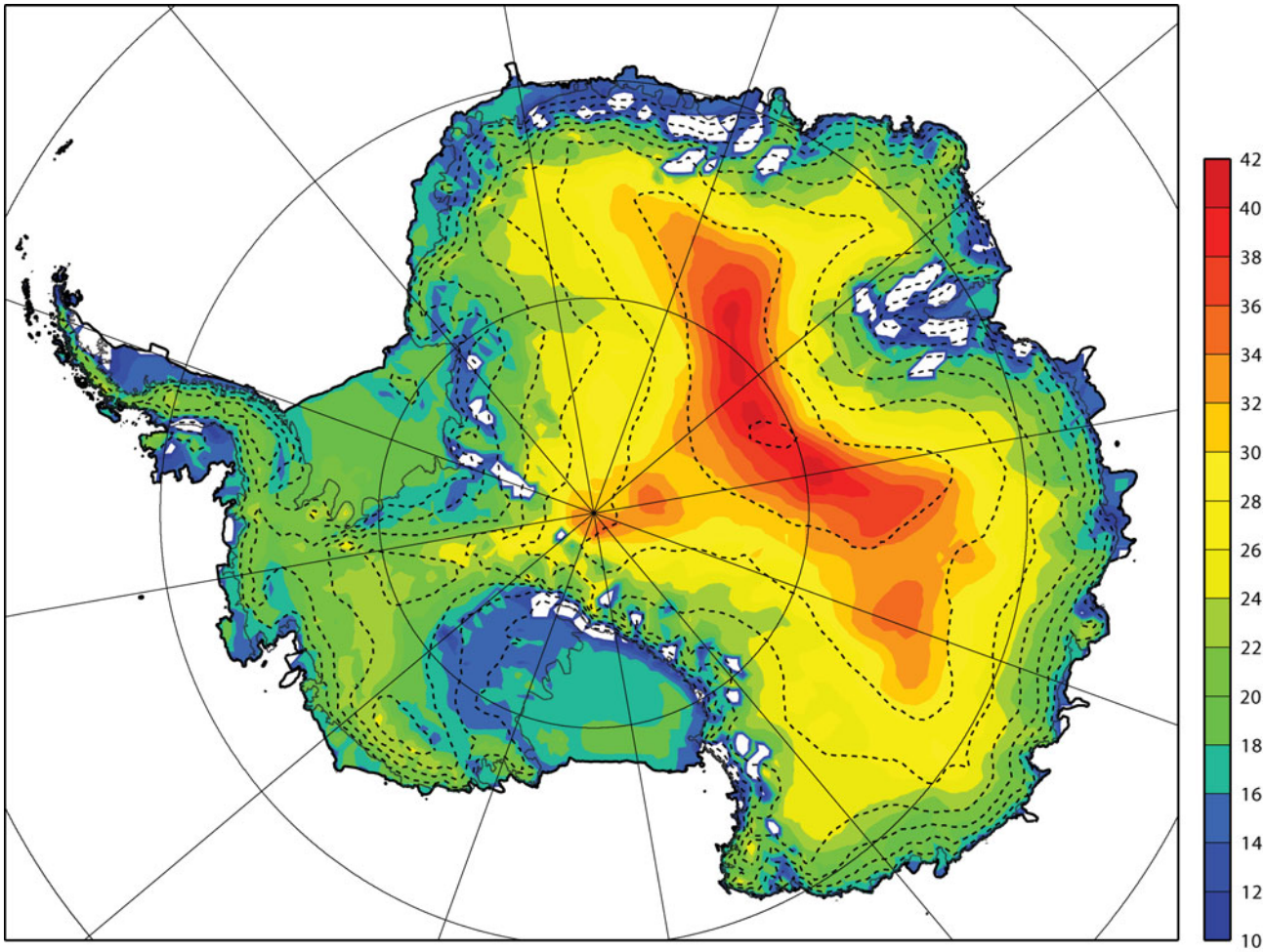

Fig. 3. Modelled firn correction depth Δh (m), defined as the height difference of the modelled firn column and an ice column of the same weight. Dashed lines are 500 m height contours, thick solid line represents the grounding line (from Vaughan 1999).

density level represents the transition from settling to sintering as the dominant densification process, the second level is the average pore close-off density. The wide range of depths is well captured by the model. The largest deviations are found for the 830 kg m^{-3} level in the dry and cold Antarctic interior, where pore close-off depths in excess of 100 m are observed. An outlier in the lower depth range is Upstream B, within the main trunk of Ice Stream B in West Antarctica (Alley & Bentley 1988). The value of 34 m at Upstream B is the lowest value observed in the dry snow zone of Antarctica. This anomalously rapid densification could be related somehow to the fact that his site is located at the upper part of the ice stream flow. A process that is neglected in the calculations is layer stretching, but this does not appear to negatively influence the results.

Figure 3 shows the distribution of the firn depth correction Δh over Antarctica. The solid line indicates the grounding line position. In the interior, slow densification results in Δh values in excess of 24 m, while in the wetter and warmer coastal region Δh values of 16–18 m are more common. Similar values are found over the large Ross and Filchner/Ronne ice shelves. Δh values show high spatial variability in the coastal zone, where the climate gradients are largest. Values clearly below 16 m are found over the more northerly ice shelves and in the Ross Sea grounding line of the West Antarctic Ice Sheet, in the region where Upstream B is situated. Similarly low Δh values are found in the relatively dry coast of Dronning Maud Land between 0 and 40°E. Values below 10 m (white in Fig. 3) occur in the periphery of ablation (blue ice) areas in Dronning Maud Land, in the Lambert Glacier Basin and along the Transantarctic Mountains.

Figure 4 presents Δh along the grounding line, plotted as a function of longitude (a) and as a frequency distribution (b). The triangles in Fig. 4a show Δh values from all model gridpoints that are intersected by the grounding line; because the climate model grid size is 55 km, the number of such points is relatively small. The small dots represent alternative Δh values that have been bilinearly interpolated from the coarser model grid to the more exact grounding

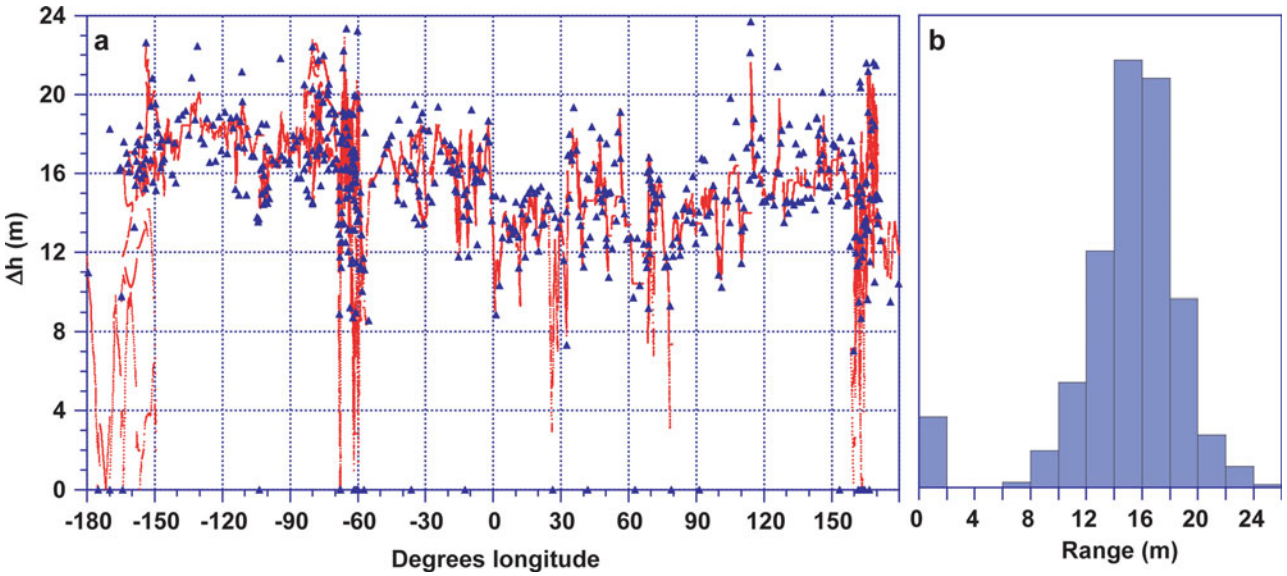

Fig. 4. Modelled firn correction depth Δh along the grounding line of the Antarctic ice sheet, **a.** as a function of longitude, both for model grid boxes that are crossed by the grounding line (triangles) as for all grounding line positions with Δh bilinearly interpolated from the climate model grid (small dots), **b.** frequency distribution of Δh.

line position. At several locations, the grounding line intersects with ablation areas (small Δh) or blue ice areas, where the entire firn layer has been removed (Δh = 0).

Apart from these downward spikes, some broad scale features are visible in Fig. 4a: generally high Δh values of 16–19 m are found along the relatively wet coasts of West Antarctica between 90 and 150°W, and lower Δh values of 12–15 m occur along the relatively dry coasts of Dronning Maud Land, Enderby Land and Mac Robertson Land (0–90°E).

Conclusions

The firn correction depth (Δh) in Antarctica is inferred from a steady-state firn densification model forced by climatology from a regional atmospheric climate model. The results show that Δh values show significant variability along the Antarctic grounding line. Incorporating these longitudinal variations of Δh will reduce the uncertainty in Antarctic solid ice fluxes. If an average value of Δh is to be used along the entire grounding line, Fig. 4b suggests that 16 ± 4 m is a reasonable choice.

The modelled density agrees well with observations from firn cores, apart from a site at the origin of fast flowing West Antarctic ice stream (Upstream B), where densification is anomalously rapid. A question that for now remains unanswered is whether the anomalously low Δh value found at Upstream B is also representative for other ice streams in Antarctica. In that case, the Δh values presented could be systematic overestimates. Other refinements that will be included in future versions of the firn model are water vapour diffusion in the firn (likely only of importance in the very dry interior) and enhanced densification due to melting (likely of importance on the coastal ice shelves, where melting occurs regularly).

References

Alley, R.B. & Bentley, C.R. 1988. Ice-core analysis on the Siple coast of West Antarctica. *Annals of Glaciology*, **11**, 1–7.

Arnaud, L., Lipenkov, V.Y., Barnola, J.-M., Gay, M. & Duval, P. 1998. Modelling of the densification of polar firn: characterization of the snow-firn transition. *Annals of Glaciology*, **26**, 39–44.

Bamber, J. & Gomez-Dans, J.-L. 2005. The accuracy of digital elevation models of the Antarctic continent. *Earth Planetary Science Letters*, **237**, 516–523.

Barnola, J.-M., Pimienta, P., Raynaud, D. & Korotkevich, Y.S. 1991. CO_2 climate relationship as deduced from the Vostok ice core: a re-evaluation of the air dating. *Tellus*, **43B**, 83–90.

Craven, M. & Allison, I. 1998. Firnification and the effects of wind-packing on Antarctic snow. *Annals of Glaciology*, **27** 239–245.

Herron, M. & Langway Jr, C. 1980. Firn densification: an empirical model. *Journal of Glaciology*, **25**, 373–385.

Kameda, T., Shoji, H., Kawada, K., Watanabe, O. & Clausen, H.B. 1994. An empirical relation between overburden pressure and firn density. *Annals of Glaciology*, **20**, 87–94.

Kaspers, K.A., van de Wal, R.S.W., van den Broeke, M.R., van Lipzig, N.P.M. & Brenninkmeijer, C.A.M. 2004. Model calculations of the age of firn air across the Antarctic continent. *Atmospheric Chemistry and Physics*, **4**, 1817–1853.

Li, J. & Zwally, H.J. 2004. Modeling the density variation in the shallow firn layer. *Annals of Glaciology*, **38**, 303–313.

Pimienta, P. & Duval, P. 1987. Rate controlling processes in the creep of polar glacier ice. *Journal de Physique*, **48**, 243–248.

Rignot, E., Bamber, J.L., van den Broeke, M.R., Davis, C., Li, Y., van de Berg, W.J. & van Meijgaard, E. 2008. Recent Antarctic mass loss from radar interferometry and regional climate modelling. *Nature Geoscience*, **2**, 106–110.

Reijmer, C.H., van Meijgaard, E. & van den Broeke, M.R. 2005. Evaluation of temperature and wind over Antarctica in a regional atmospheric climate model. *Journal of Geophysical Research*, **110**, 10.1029/2004JD005234.

Spencer, M.K., Alley, R.B. & Creyts, T.T. 2001. Preliminary firn-densification model with 38-site dataset. *Journal of Glaciology*, **47**, 671–676.

Van Lipzig, N.P.M., Turner, J., Colwell, S.R. & van den Broeke, M.R. 2004. The near-surface wind field over the Antarctic continent. *International Journal of Climatology*, **24**, 1973–1982.

Van de Berg, W.J., van den Broeke, M.R., van Meijgaard, E. & Reijmer, C.H. 2006. Reassessment of the Antarctic surface mass balance using calibrated output of a regional atmospheric climate model. *Journal of Geophysical Research*, **111**, 10.1029/2006JD007127.

Van den Broeke, M.R. 2008. Depth and density of the Antarctic firn layer. *Arctic, Antarctic and Alpine Research*, **40**.

Van den Broeke, M.R., van de Berg, W.J., van Meijgaard, E. & Reijmer, C.H. 2006. Identification of Antarctic ablation areas using a regional atmospheric climate model. *Journal of Geophysical Research*, **111**, 10.1029/2006JD007127.

Vaughan, D.G., Bamber, J.L., Giovinetto, M. & Cooper, A.P.R. 1999. Reassessment of net surface mass balance in Antarctica. *Journal of Climatology*, **12**, 933–946.

Winther, J.-G., Jespersen, M.N. & Liston, G.E. 2001. Blue-ice areas in Antarctica derived from NOAA AVHRR satellite data. *Journal of Glaciology*, **47**, 325–334.

Zwally, H.J., Giovinetto, M.B., Li, J., Cornejo, H.G., Beckley, M.A., Brenner, A.C., Saba, J.L. & Yi, D. 2005. Mass changes of the Greenland and Antarctic ice sheets and shelves and contributions to sea-level rise: 1992–2002. *Journal of Glaciology*, **51**, 509–527.